

# Mechanical Properties and Dimensional Effects of ZnO- and SnO<sub>2</sub>-Based Varistors

Miguel Angel Ramírez,<sup>†,‡</sup> Fernando Rubio-Marcos,<sup>§</sup> José Francisco Fernández,<sup>§</sup> Markus Lengauer,<sup>¶</sup>  
Paulo Roberto Bueno,<sup>‡</sup> Elson Longo,<sup>‡</sup> and José Arana Varela<sup>‡</sup>

<sup>‡</sup>Universidade Estadual Paulista, UNESP, Instituto de Química, Araraquara, SP, Brazil

<sup>§</sup>Electroceramic Departament, Instituto de Cerámica y Vidrio, 28049 Madrid, Spain

<sup>¶</sup>Department of Automotive Engineering, University of Applied Sciences, 8020 Graz, Austria

A comparison between traditional ZnO-(modified Matsuoka system, [ZnO]) and SnO<sub>2</sub>-based varistors (98.9%SnO<sub>2</sub>+1%CoO+0.05%Nb<sub>2</sub>O<sub>5</sub>+0.05%Cr<sub>2</sub>O<sub>3</sub>, [SCNCR]) regarding their mechanical properties, finite element (FE) modeling, and macroscopic response with current pulse is presented in this work. The experimental values of the elastic (static and dynamic) modulus and bending strength are given. Both the static and the dynamic modulus were two times higher for SnO<sub>2</sub> (~200 GPa) with respect to ZnO (~100 GPa). A similar behavior was found for the bending strength, confirming the superior mechanical properties of SCNCR associated with a homogeneous microstructure. The finite element analyses yielded the most appropriate thickness/diameter aspect ratio ( $H/D$ ), while thermomechanical stress is minimized. The values of ( $H/D$ ) were lower for the SCNCR in comparison with the ZnO-based varistors, allowing the production of smaller pieces that can resist the same thermomechanical stress. Finally, preliminary analyses of the macroscopic failures for samples treated with degradation pulses of 8/20- $\mu$ s type allowed to confirm the absence of failures due to cracking and/or puncture in the SCNCR. The absence of these failures originates from the good thermomechanical properties.

## I. Introduction

VARISTORS are materials whose resistance varies with the applied electric field, resulting in nonohmic  $I$ - $V$  characteristics.<sup>1</sup> This property allows their use in the protection of electric and electronic circuits, whereas lightning rods remain the principal application.<sup>2</sup> The varistors inside the lightning rods experience a high compression stress when all the elements of the device are kept close together (to provide a good electrical contact between the single pieces). This aspect is critical for varistors, specifically for ZnO-based varistors forming piezoelectric crystals that are significantly deformed under the action of electric fields.<sup>3</sup> These deformations translate to regions inside the varistor with different stress. The characterization of the mechanical properties of this material is an important subject, and still little studied in the literature.<sup>3</sup> In this work, the experimental values of the static ( $E_s$ ) and dynamic ( $E_d$ ) modulus and bending strength ( $\sigma_f$ ) are given that can be related to the thermomechanical failure types such as cracking and/or puncture.<sup>4–6</sup>

The mechanical properties were treated as changeable at the beginning of the analysis of the effect of the  $H/D$  ratio on the mechanical tensions using the FE analyses. Lengauer *et al.*<sup>7</sup> studied exactly this problem for ZnO-based varistors. Within

this model, the increase in temperature  $T$  at the time  $t$ , caused by the Joule heating, is given by

$$T(t) = T_0 + \frac{1}{m \cdot c_v} \int_0^t P(\tau) d\tau, \quad (1)$$

where  $T_0$  is the uniform initial temperature of the varistor (taken to be 25 °C) at  $t = 0$ ,  $m$  is the mass,  $c_v$  is the specific heat capacity at a constant volume, and  $P$  is the electric power. Because of the heating and the thermal expansion coefficient ( $\epsilon$ ), the varistor tends to expand. But the heating process is so rapid that the mass forces (inertia) prevent quick thermal expansion. This leads to an overall compressive stress state in the varistor in the first phase.<sup>7</sup> This can be seen as the excitation that causes the varistor to vibrate, which depends on its geometry. As a consequence, tensile stresses, which are much more detrimental to ceramics, also arise.<sup>3–6</sup> Thus, wave interaction, either constructive or deconstructive, occurs inside the varistor. A classical approach based on the wave differential equation, to determine when, where, and with which amplitude the maximum tensile stress can be expected, appears to be an impossible task. Therefore, numerical analysis was chosen as an appropriate method.<sup>7</sup> There are some studies on the dimensional effect of SnO<sub>2</sub>-<sup>8–9</sup> and ZnO-based varistors<sup>10</sup> on electric properties not considering the mechanical behavior.

For ZnO-based varistors, the phenomena of pulse degradation have been widely studied<sup>11–13</sup>; however, for varistors of the SnO<sub>2</sub> system there are still no analyses. This subject is of great importance in order to apply these materials commercially in lightning rods. In this letter, we present preliminary results of the degradation behavior of ZnO- and SnO<sub>2</sub>-based varistors treated with pulses and its correlation with the thermomechanical properties.

## II. Experimental Procedure

The investigated ceramic varistors correspond to the following systems: the Modified Matsuoka system<sup>14</sup>: 95.4%ZnO+1.5% Sb<sub>2</sub>O<sub>3</sub>+1%NiO+0.1%SiO<sub>2</sub>+0.5% (Bi<sub>2</sub>O<sub>3</sub>, SnO<sub>2</sub>, Co<sub>2</sub>O<sub>3</sub>, MnO) [ZnO] and the Pianaro system<sup>15</sup>: 98.9%SnO<sub>2</sub>+1%CoO+0.05%Nb<sub>2</sub>O<sub>5</sub>+0.05%Cr<sub>2</sub>O<sub>3</sub> (SCNCR), all percentages in mol%. The powders were prepared by the mixed oxide route and pressed uniaxially to obtain rectangular plates. The samples of the ZnO-based varistors were sintered at 1180 °C for 2 hours and those of the SCNCR at 1300 °C for 1 hour. The density of the sintered bodies ( $\rho$ ) was determined by the Archimedes method. The polished surfaces of both system samples were investigated using scanning electron microscopy (SEM, Zeiss DSM 940 A, Oberkochen, Germany). Six bars of each system were cut from sintered samples using an automatic cutting machine with

M.-J. Pan—contributing editor

Manuscript No. 24529. Received April 10, 2008; approved May 22, 2008.

<sup>†</sup>Author to whom correspondence should be addressed. e-mail: margbrasil@yahoo.com

diamond saw disks with water as a refrigerant. Cut samples were polished with diamond to avoid the presence of surface defects. The final dimensions of the bars were  $60 \times 4 \times 3$  mm as specified by international norms.<sup>16</sup>  $E_s$  and  $\sigma_f$  were determined from the tension–deformation curve ( $\sigma$  vs  $\delta$ ) by means of a stress test in three points using a Universal INSTRON 4411 (Warren, MI) equipment.  $\sigma_f$  was determined from the maximum charge considering the sample geometry.  $E_d$  was measured using a resonance technique that uses the eigenfrequency of vibration (related to  $E_d$ ) using a GrindoSonic MK5 (Leuven, Belgium) equipment. After this mechanical characterization, an FE-analysis was performed to find the optimum aspect ratio  $H/D$  for each of the three volume sizes that led to minimal thermomechanical stress in the varistors. These volumes were chosen considering critical  $A/V$  ratios from studies already reported in the literature.<sup>8–9</sup> For each volume size, the aspect ratio was varied in the calculations between 0.05 and 1.5 in steps of 0.05. In order to resolve all of the relevant mode shapes accurately, the element size has to be adapted to the highest eigenfrequency  $\nu_{\max}$ . The element's (square-shaped 2-D) size was chosen to be  $1/20$  of the smallest wavelength  $\lambda_{\min} = c/D_{\max}$ . The speed of sound  $c$  is calculated by  $(E/\rho)^{1/2}$ , with  $E$  being the elastic modulus and  $\rho$  the density. Because of the varying aspect ratio, a modal analysis was performed first for each combination of material/volume/aspect ratio to obtain the eigenfrequencies of interest, especially  $\nu_{\max}$ . Equation (1) was applied to introduce the temperature. The calculation was performed until an end time of 100  $\mu$ s, which is sufficient for finding the maximum tensile stress. Finally, samples with the same volumes as used for the FE analyses were prepared for the analysis of the thermomechanical behavior during degradation with 8/20  $\mu$ s-type current pulses. The degradation tests had been carried out by means of a current generator adapted from a Haefely instrument that delivers 8/20  $\mu$ s current pulses. The response of the devices was registered with a Tektronix (Taiwan; 8 bits, 100 MHz) digital oscilloscope.<sup>17</sup>

### III. Results and Discussion

In Fig. 1, the curves  $\sigma$  vs  $\delta$  for selected varistor samples based on ZnO and SnO<sub>2</sub> are given. The relation  $\sigma$  vs  $\delta$  is nonlinear in the beginning of the plot range; the distortion observed at low load is associated with support adjustment.  $E_s$  was calculated by means of the ratio between  $\sigma$  and  $\delta$  in the linear elastic region, where  $\delta$  is totally reversible and proportional to the  $\sigma$ . In Table I, the values of  $E_s$ ,  $E_d$ , and  $\sigma_f$  are given and it was found that the values for the SCNCr system are approximately twice the values of the ZnO system. The excellent mechanical behavior of the SCNCr system is associated with the high density of the sintered bodies and with the microstructural homogeneity, due to the characteristic single-phase grain matrix microstructure of these ceramics (Fig. 1, inset). In comparison, the multiphase ZnO-based varistor possesses a large grain size ( $d = 8.5$   $\mu$ m) with secondary crystalline grains of the spinel phase and the remaining liquid phase surrounding the grains and filling triple point junctions.<sup>1,11</sup> The mechanical fracture, once initiated, proceeds pref-

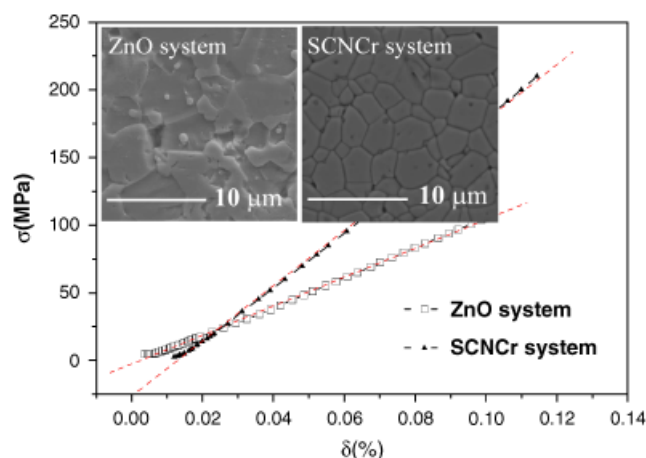


**Fig. 1.**  $\sigma$  vs  $\delta$  curves for the ZnO and 98.9%SnO<sub>2</sub>+1%CoO+0.05% Nb<sub>2</sub>O<sub>5</sub>+0.05%Cr<sub>2</sub>O<sub>3</sub> (SCNCr) varistors system. Secondary-electron images of polished samples of sintered ZnO and SCNCr systems (inset).

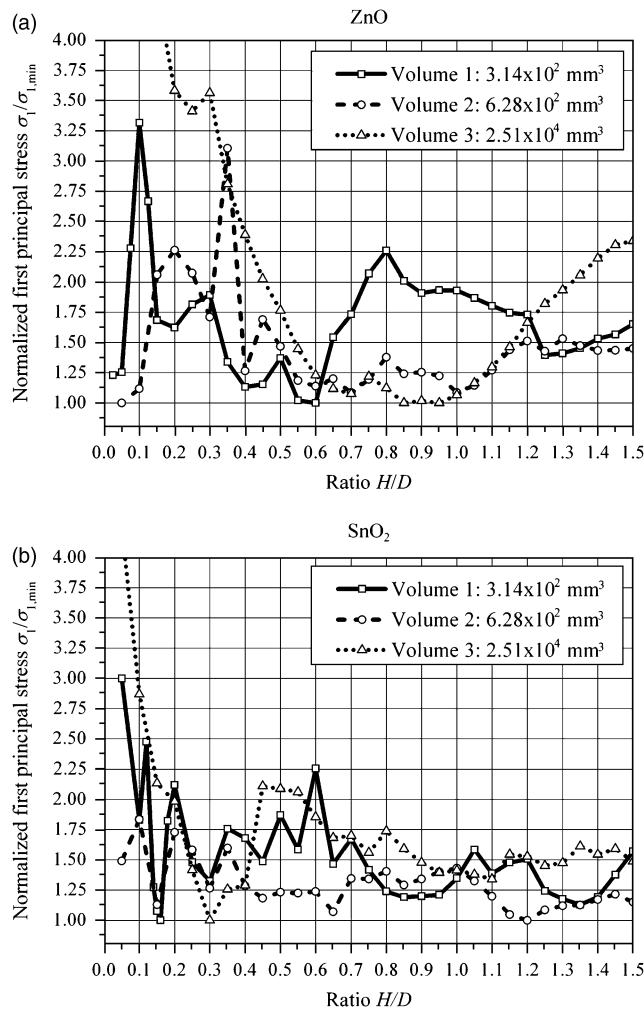
erentially through the secondary phases and the large bismuth-spinels readily give rise to easy crack paths.<sup>3</sup> These results, together with the excellent thermal conductivity of the SCNCr system reported in Bueno *et al.*,<sup>18</sup> allow to predict a good thermomechanical behavior and the possibility to manufacture varistor parts with smaller dimensions fulfilling the same electric and mechanical requirements. To confirm this, an FE-analysis using the experimental values of  $E_s$ ,  $E_d$ , and  $\sigma_f$  was performed to determine the  $H/D$  ratio that would minimize the mechanical stresses.

Fig. 2(a) and (b) show the influence of the  $H/D$  ratio on the main mechanical stresses for varistors of the ZnO and SnO<sub>2</sub> systems, respectively. The vertical axis represents the normalized tensions (maximum principal stresses divided by the minimum principal stresses) and the horizontal axis represents the  $H/D$  ratio. From the graphs, the influence of the  $H/D$  ratio on the mechanical tensions for both systems is clear, showing that the dependence is stronger in the case of the ZnO system. The variation of the tensions with the  $H/D$  ratio is higher for small volumes. This effect could be associated with the same order of magnitude of the stress-wave length and the varistor's main dimension with wave reflections on the varistor's boundaries. For instance, from Fig. 2(a), a sample with  $3.14 \times 10^2$  mm<sup>3</sup> volume and  $H/D = 0.1$  would be subjected to a tension 3.25 times higher than a sample with  $H/D = 0.6$ . In Table I,  $H/D$  values that minimize the mechanical tension are reported. The optimal  $H/D$  ratio for a volume of  $2.51 \times 10^4$  mm<sup>3</sup> is 0.85 and/or 0.95, and values close to 0.9 were also found by Lengauer *et al.*<sup>7</sup> for ZnO-based varistors with  $4.0 \times 10^4$  mm<sup>3</sup> volume. For extreme volumes ("lowers" and "highers"), the  $H/D$  ratio for the SCNCr system is lower ("0.15" and "0.3"); however, for intermediate volumes, the result is the opposite (0.65). This result indicates that for varistor ceramics with a high volume, it is more recommendable to increase the diameter than the thickness, which

**Table I.** Thermomechanical Properties and Results of the FE-Analyses for ZnO and SCNCr System

Varistor system	Thermomechanical properties							FE analysis		
	$E_s$ (GPa)	$E_d$ (GPa)	$\sigma_f$ (MPa)	Density (Kg·m <sup>-3</sup> )	$d^f$ ( $\mu$ m)	$\alpha^{\ddagger}$ (K <sup>-1</sup> )	$c_v^{\S}$ (J·Kg <sup>-1</sup> ·K <sup>-1</sup> )	Volume <sup>§</sup> (mm <sup>3</sup> )	Max. tension $\sigma_I$ (MPa)	$H/D$
ZnO	116 ± 14	120 ± 2	106 ± 3	5648	8.5	7.10 <sup>-6</sup>	530	$3.14 \times 10^{2(1)}$	82	0.60
								$6.28 \times 10^{2(2)}$	5	1.0
								$2.51 \times 10^{4(3)}$	4	0.85–0.95
								$3.14 \times 10^2$	54	0.15
SCNCr	212 ± 6	251 ± 3	207 ± 5	6900	4.5	2.10 <sup>-6</sup>	370	$6.28 \times 10^2$	10	0.65
								$2.51 \times 10^4$	3	0.30

<sup>†</sup>Average grain size values determined by scanning electron microscopy utilizing the intercept method. <sup>‡</sup>Values taken from the Bueno *et al.*<sup>18</sup> <sup>§</sup>Volumes corresponding to samples with: (1) diameter ( $D$ ) = 20 mm and thickness ( $H$ ) = 1 mm, (2)  $D$  = 20 mm,  $H$  = 2 mm, (3)  $D$  = 40 mm,  $H$  = 20 mm.



**Fig. 2.** FE-analysis of the dependence of the maximum tensile stress on the  $H/D$  ratio for: (a) ZnO and (b) 98.9%SnO<sub>2</sub>+1%CoO+0.05%Nb<sub>2</sub>O<sub>5</sub>+0.05%Cr<sub>2</sub>O<sub>3</sub> system.

would also improve the capacity of the energy dissipation, specifically for the SCNCr system that is microstructurally homogeneous. However, the optimum  $H/D$  ratio does not show any correlation to the volume of the varistor. In fact, for each volume value, the optimum  $H/D$  ratio has to be determined separately.

The nonohmic characteristics of both systems before the degradation process are shown in Fig. 3 and the varistor parameters are listed in Table II. The values for electrical breakdown field ( $E_b$ ), leakage current ( $I_l$ ), and nonlinear coefficient ( $\alpha$ ) are in agreement with the literature.<sup>14–15</sup> The comparative analyses of the degradation mechanisms with pulse applications will be the subject of a separate study. However, preliminary results show that after pulse application the ZnO-based varistors, show failures such as partial fusing of the electrodes, cracking, and puncture as can be seen from Fig. 3(a) (inset). In contrast, samples of the SCNCr system do not show thermomechanical failures as can be seen from Fig. 3(b) (inset). Eda<sup>4</sup> and Voltja *et al.*<sup>5</sup> proposed that for ZnO-based varistors, pulses of duration  $>100$   $\mu$ s cause failures due to puncture and pulses of duration  $<50$   $\mu$ s cause failures due to cracking. Recently, Ramírez *et al.*<sup>11</sup> have shown that pulses of a long duration such as 2 ms affect both failure types in ZnO-based varistors. Our results show that ZnO-based varistors, after degradation with short pulses, also show both failure types, indicating that the failure type in metal oxide varistors is related to the chemical composition, microstructural, and thermomechanical properties, and not to the duration of the pulse as proposed initially.<sup>4–5</sup> The ZnO-based varistor showed a PTCR effect<sup>19</sup> in which the current amplitude decreased with successive current pulse applications, and Joule heating of the

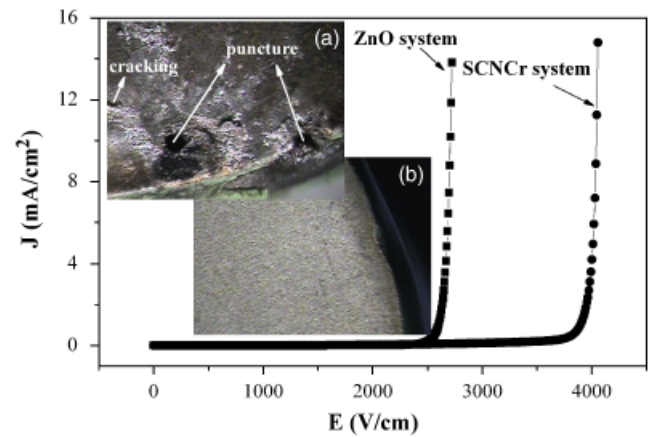


**Fig. 3.**  $J$ - $E$  characteristics for the ZnO and 98.9%SnO<sub>2</sub>+1%CoO+0.05%Nb<sub>2</sub>O<sub>5</sub>+0.05%Cr<sub>2</sub>O<sub>3</sub> (SCNCr) varistor system. Inset, samples after degradation with 8/20  $\mu$ s pulses: (a) Failure by cracking and puncture in the ZnO-based varistors (magnification  $\times 40$ ). (b) SCNCr system free from failures (magnification  $\times 40$ ).

**Table II.** Nonohmic Properties before the Degradation Process of the ZnO and SCNCr System

Varistor system	$E_b$ (V/cm)	$I_l$ ( $\mu$ A)	$\alpha^\dagger$
ZnO	2600	1.3	56
SCNCr	3900	1.0	65

<sup>†</sup>Values calculated from 1 to 10 mA/cm<sup>2</sup>.

samples could manifest itself through an increase in grain resistance, leading to currents that decrease for a constant applied voltage.<sup>20</sup> The use of varistors with better thermomechanical properties could contribute toward minimizing the above-mentioned PTCR effect and its adverse effect on varistor stability.

#### IV. Conclusions

The varistors of the SCNCr system possess superior thermomechanical properties (values of  $E_s$ ,  $E_b$ ,  $\sigma_f$ , and thermal conductivity) that correspond approximately to double the values found for the ZnO-based varistors due to the homogeneous microstructure. FE analyses showed that the  $H/D$  ratios, which minimize the mechanical stress, are lower in the SCNCr system due to the better thermomechanical behavior. This would allow manufacture of pieces with smaller dimensions fulfilling the same mechanical requirements. Preliminary studies of the varistor behavior regarding the degradation phenomena with 8/20  $\mu$ s current pulses show that the SCNCr system is free from cracking and/or puncture-type failures due to good thermomechanical properties. ZnO-based varistors show both failure types for long pulses<sup>11</sup> as well as for short pulses (8/20  $\mu$ s). These results allow to state that the failure type is associated with the thermomechanical behavior of the varistors and not the duration of the pulses. The use of varistors with better thermomechanical properties would contribute toward minimizing the PTCR effect and its adverse effect on varistor stability.

#### Acknowledgments

The authors gratefully acknowledge the financial support of the Brazilian financing agency FAPESP, Program CYTED (Project PI-VIII.13 PROALERTA).

#### References

- D. R. Clarke, "Varistor Ceramics," *J. Am. Ceram. Soc.*, **82** [3] 485–502 (1999).
- M. A. Ramirez, A. Z. Simões, P. R. Bueno, M. A. Márquez, M. O. Orlandi, and J. A. Varela, "Importance of Oxygen Atmosphere to Recover the ZnO-based Varistors Properties," *J. Mater. Sci.*, **41**, 6221–7 (2006).

- <sup>3</sup>B. Balzer, M. Hagemeister, P. Kocher, and L. J. Gauckler, "Mechanical Strength and Microstructure of Zinc Oxide Varistor Ceramics," *J. Am. Ceram. Soc.*, **87** [10] 1932–8 (2004).
- <sup>4</sup>K. Eda, "Destruction Mechanism of ZnO Varistor Due to High Currents," *J. Appl. Phys.*, **56** [10] 2948–55 (1984).
- <sup>5</sup>A. Vojta and D. R. Clarke, "Electrical-Impulse-Induced Fracture of Zinc Oxide Varistor Ceramics," *J. Am. Ceram. Soc.*, **80** [8] 2086–92 (1997).
- <sup>6</sup>J. L. He and J. Hu, "Discussions on Nonuniformity of Energy Absorption Capabilities of ZnO Varistors," *IEEE Trans. Pow. Delv.*, **22** [3] 1523–32 (2007).
- <sup>7</sup>M. Lengauer, D. Rubeša, and R. Danzer, "Finite Element Modelling of the Electrical Impulse Induced Fracture of High Voltage Varistors," *J. Eur. Ceram. Soc.*, **20**, 1017–21 (2000).
- <sup>8</sup>M. A. Ramírez, W. Bassi, R. Parra, P. R. Bueno, E. Longo, and J. A. Varela, "Comparative Electrical Behavior at Low and High-Current of SnO<sub>2</sub> and ZnO-based Varistors," *J. Am. Ceram. Soc.*, doi: 10.1111/j.1551-2916.2008.02436.x.
- <sup>9</sup>M. A. Ramírez, J. F. Fernández, M. de la Rubia, J. de Frutos, P. R. Bueno, E. Longo, and J. A. Varela, "The Influence of Area/Volume Ratio on Microstructure and Non-Ohmic Properties of SnO<sub>2</sub>-Based Varistors Ceramics Blocks," *J. Mater. Sci.: Mater. Electron.*, doi: 10.1007/s10854-008-9602-8 (2008).
- <sup>10</sup>S. T. Li, J. Y. Li, F. Y. Liu, M. Alim, and G. Chen, "The Dimensional Effect of Breakdown Field in ZnO Varistors," *J. Phys. D: Appl. Phys.*, **35** [7] 1884–8 (2002).
- <sup>11</sup>M. A. Ramírez, P. R. Bueno, W. C. Ribeiro, D. A. Bonetti, J. M. Villa, M. A. Márquez, J. A. Varela, and C. R. Rojo, "The Failure Analyses on ZnO Varistors Used in High Tension Devices," *J. Mat. Sci.*, **40**, 5591–6 (2005).
- <sup>12</sup>M. A. Ramírez, A. Z. Simões, M. A. Márquez, Y. Maniette, A. A. Cavalheiro, and J. A. Varela, "Characterization of ZnO-degraded Varistors Used in High-Tension Devices," *Mat. Res. Bull.*, **42**, 1159–68 (2007).
- <sup>13</sup>M. A. Ramírez, P. R. Bueno, J. A. Varela, and M. A. Márquez, "Degradation and Recovery of ZnO Varistors," *Bol. Soc. Esp. Ceram. Vid.*, **45**, 346–51 (2006).
- <sup>14</sup>M. Matsuoka, "Nonohmic Properties of Zinc Oxide Ceramics," *Jap. J. Appl. Phys.*, **10**, 736–46 (1971).
- <sup>15</sup>S. A. Pianaro, P. R. Bueno, E. Longo, and J. A. Varela, "A New SnO<sub>2</sub>-Based Varistor System," *J. Mat. Sci. Lett.*, **14**, 692–4 (1995).
- <sup>16</sup>ASTM International. ASTM C 1259 Standard Test Method for Dynamic Young's Shear Modulus and Poisson's Ratio by Impulse Excitation of Vibration. Designation E 1876–99 (2008).
- <sup>17</sup>M. A. Ramírez, W. Bassi, P. R. Bueno, E. Longo, and J. A. Varela, "Comparative Degradation of ZnO- and SnO<sub>2</sub>-based Polycrystalline Non-Ohmic Devices by Current Pulse Stress," *J. Phys. D: Appl. Phys.*, **41**, 122002 (2008).
- <sup>18</sup>P. R. Bueno, J. A. Varela, C. M. Barrado, E. Longo, and E. R. Leite, "A Comparative Study of Thermal Conductivity in ZnO and SnO<sub>2</sub>-Based Varistor Systems," *J. Am. Ceram. Soc.*, **88** [9] 2629–31 (2005).
- <sup>19</sup>D. Fernandez-Hevia, J. de Frutos, A. C. Caballero, and J. F. Fernandez, "Bulk-Grain Resistivity and Positive Temperature Coefficient of ZnO-Based Varistors," *Appl. Phys. Lett.*, **82** [2] 212–4 (2003).
- <sup>20</sup>F. A. Modine and R. B. Wheeler, "Pulse Response Characteristics of ZnO Varistors," *J. Appl. Phys.*, **67** [10] 6560–6 (1990). □